Virus Research 355 (2025) 199564

Contents lists available at ScienceDirect

Virus Research

journal homepage: www.elsevier.com/locate/virusres

Identification of host specificity determinants in brome mosaic virus for rice infection

Yifan Zhang, Masanori Kaido [1], Akira Mine, Yoshitaka Takano, Kazuyuki Mise [*]

Laboratory of Plant Pathology, Graduate School of Agriculture, Kyoto University, Kyoto 606-8502, Japan

ARTICLE INFO

Keywords:
Brome mosaic virus
Host specificity
Rice
Systemic infection
RNA polymerase
Intrinsic disordered region

ABSTRACT

Brome mosaic virus (BMV) is a tripartite positive-stranded RNA plant virus. The genomic RNA2 encodes the 2a protein, which has conserved RNA-dependent RNA polymerase motifs and is required for viral RNA replication. In this study, we have used two BMV strains, F and KU5, and identified two key amino acid residues, 776R and 784T, in the C-terminal non-conserved region of the 2a protein that are critical for systemic infection of BMV-F in rice. While KU5 strain was not able to systemically infect rice, the KU5 mutant strain with two codon changes for 776R and 784T in the 2a gene gained the ability to establish systemic infection in rice, which affects long-distance movement, but not replication or cell-to-cell movement. Through infection assays of KU5 synonymous mutant strains, we demonstrated that amino acids, rather than RNA sequences or secondary structures, are responsible for viral infectivity in rice. Computer predictions and yeast two-hybrid screening revealed that the C-terminal region of 2a functions as an intrinsically disordered region, capable of interacting with host proteins. These results provide molecular insights into the host specificity of BMV and advance our understanding of RNA virus evolution and host-pathogen interactions.

1. Introduction

Brome mosaic virus (BMV) is a positive-stranded RNA virus belonging to the genus *Bromovirus* of the family *Bromoviridae*. It is also a typical member of the alphavirus-like superfamily, which is characterized by similar genome structures (He et al., 2021). BMV has many strains and infects a wide range of plant hosts, including barley, maize, rice, and wheat, causing symptoms such as mosaic patterns, chlorosis, and stunted growth. In wheat, infection results in reduced plant height and tiller production, and can reduce grain yield by up to 61% (Hodge et al., 2019).

BMV has been used as a model to study gene expression, RNA replication, virus-host interactions, recombination, and encapsidation of positive-strand RNA viruses (Trzmiel et al., 2023). The BMV genome consists of tripartite RNAs designated RNA1 (3.2 kb), RNA2 (2.9 kb), and RNA3 (2.1 kb). RNA1 and RNA2 encode non-structural proteins 1a (104-kDa) and 2a (94-kDa), respectively (Ahlquist et al., 1984). RNA3 encodes the 3a (32-kDa) non-structural protein and the coat protein (CP; 20-kDa), which are required for cell-to-cell and long-distance movement in plants (Allison et al., 1990; Mise & Ahlquist, 1995; Sacher & Ahlquist, 1989). CP is translated from subgenomic RNA4, which is synthesized from negative-strand RNA3 (Miller et al., 1985).

The central region of the BMV 2a protein contains a conserved RNA-dependent RNA polymerase (RdRp) domain that is essential for viral RNA synthesis (Kamer & Argos, 1984). The N-terminal region of the BMV 2a protein is involved in interacting with the 1a replication protein within the viral replication complex (VRC), which is anchored to the perinuclear endoplasmic reticulum (nER) membrane (Chen et al., 2000). This interaction is critical for the recruitment of 2a to the VRC, allowing the formation of a functional replication complex (Schwartz et al., 2002). In addition to its essential role in viral RNA replication, studies have shown that the C-terminal region of the BMV 2a protein also influences the systemic spread of the virus in barley (Traynor et al., 1991). However, the exact amino acid residues responsible for this function and the underlying molecular mechanism, remain poorly understood.

In this study, we identified two key amino acid residues, 776R and 784T, in the C-terminal region of the BMV 2a protein that are essential for systemic infection in and adaptation to rice. While the parental KU5

Nucleotide sequence data for BMV is available in the GenBank database under accession numbers PV173122, PV173123, and PV173124 for clones pB2KU52, pB1KU51, and pB3KU53, respectively.

* Corresponding author.
E-mail address: mise.kazuyuki.3x@kyoto-u.ac.jp (K. Mise).
[1] Present address: Laboratory of Plant Environmental Microbiology, Graduate School of Agriculture, Setsunan University, Hirakata 573-0101, Japan.

https://doi.org/10.1016/j.virusres.2025.199564
Received 28 February 2025; Received in revised form 21 March 2025; Accepted 23 March 2025
Available online 25 March 2025

strain was unable to systemically infect rice, the KU5 mutant strain with two codon changes for 776R and 784T in the 2a gene acquired the ability to establish systemic infection in rice. By introducing synonymous mutations, we provided evidence that amino acid changes, rather than RNA sequence changes, are primarily driver of this shift in rice infectivity. *In silico* protein structure predictions and yeast two-hybrid screening further revealed that the C-terminal 2a region functions as an intrinsically disordered region (IDR) capable of interacting with host factors. These findings provide molecular insights into the role of BMV RNA2 in host specificity and systemic infection, contributing to a better understanding of viral adaptation and movement mechanisms.

2. Materials and methods

2.1. Plant materials and growth conditions

Seeds of rice (*Oryza sativa*) cv. Habataki were provided from Dr. Teraishi, Laboratory of Plant Breeding, Graduate School of Agriculture, Kyoto University (GSAKU). The seeds of *Chenopodium quinoa* (line Kd) and barley (*Hordeum vulgare*) cv. Hinodehadaka were propagated in the Laboratory of Plant Pathology, GSAKU. Rice plants were grown at 25°C, and *C. quinoa* and barley plants were grown at 23°C with 16 hours of illumination per day.

2.2. BMV strains

The BMV PV47 strain was obtained from the American Type Culture Collection (ATCC, Manassas, VA, USA). T7 RNA polymerase transcripts from three plasmids, pB1KU51, pB2KU52 and pB3KU53 described below are collectively defined as the KU5 strain of BMV. The BMV-F strain was derived from the Fescue strain of BMV (Ding et al., 2006), kindly provided by Professor Richard S. Nelson, The Samuel Noble Foundation, OK, USA and recloned as below.

2.3. Plasmid constructs

All plasmids described below were constructed by recombinant PCR using KOD One PCR Master Mix (Toyobo, Japan) or ligation using restriction enzyme digested fragments. All primers used in this study are listed in Supplementary Table S1. The nucleotide sequences of the fragments amplified by PCR were checked to confirm that only desired mutations were introduced. All cDNA plasmids were linearized with *Eco*RI and capped viral RNA transcripts were synthesized as previously described (Kroner & Ahlquist, 1992). The transcript from the plasmid containing the RNA2 variant is referred to by its plasmid name without the prefix 'p'. For example, RNA2 produced from pB2FK2^{E} is referred to as B2FK2^{E}.

2.3.1. pB1KU51, pB2KU52 and pB3KU53

First strand cDNA of all three genomic RNAs of BMV PV47 strain was primed with primer B123-E. Primer B123-E anneals to the 3′-terminal 17 nucleotides of all BMV M1 strain RNAs (Ahlquist et al., 1984) and contains an additional 5′ sequence defining an *Eco*RI restriction site. Double-stranded cDNAs were amplified by RT-PCR using the first-stranded cDNAs as templates. The RNA1 cDNA was amplified using primer B1-5P and primer B123-E, the RNA2 cDNA was amplified using primer B2-5P and primer B123-E, and the RNA3 cDNA was amplified using primer B3-5P and primer B123-E. Primers B1-5P, B2-5P and B3-5P correspond to the 5′-terminal sequences of RNA1, RNA2 and RNA3 of BMV M1 strain, respectively, and contain additional 5′ bases defining a *Pst*I restriction site and a T7 RNA polymerase promoter sequence. Amplified cDNA fragments of RNA1, RNA2 and RNA3 of BMV PV47 strain were digested with *Pst*I and *Eco*RI, and then inserted into the *Pst*I-*Eco*RI site of pUC119 (Takara, Japan), to construct pB1KU51, pB2KU52 and pB3KU53, respectively.

2.3.2. pB1KN1, pB2KN2 and pB3KN3

To facilitate the cloning of hybrids between the two BMV strains, SP6-based transcription vectors were modified to T7-based. Full-length cDNA inserts from pF1-11, pF2-2 and pF3-5 of the BMV Fescue strain (Ding et al., 2006) were transferred into T7-based plasmids, to generate pB1KN1, pB2KN2 and pB3KN3, respectively. Each cDNA insert was PCR amplified from the three pF plasmids using a set of the 5' terminal primers B1-5P, B2-5P and B3-5P and the 3' terminal primer B123-E. Amplified fragments were digested with *Pst*I and *Eco*RI and ligated into the *Pst*I-*Eco*RI site of pUC119 (Takara, Shiga, Japan), to generate pB1KN1, pB2KN2 and pB3KN3, respectively.

2.3.3. pB2FK2^{E}, pB2KF2^{E}, pB2FK2^{ES} and pB2KF2^{S}

A small DNA fragment of pB2KN2 digested with *Eco*RI and *Eco*RV was used to replace the corresponding region of pB2KU52, to generate pB2FK2^{E}. A small DNA fragment of pB2KU52 digested with *Eco*RI and *Eco*RV was used to replace the corresponding region of pB2KN2, to generate pB2KF2^{E}. A small DNA fragment of pB2KN2 digested with *Eco*RV and *Sac*I was used to replace the corresponding region of pB2KU52, to generate pB2FK2^{ES}. A small DNA fragment of pB2KN2 digested with *Eco*RI and *Sac*I was used to replace the corresponding region of pB2KU52, to generate pB2KF2^{S}.

2.3.4. pB2KU52^{776R}, pB2KU52^{776R2}, pB2KU52^{776R4}, pB2KU52^{776R5}

DNA fragments were amplified by PCR from pB2KU52 using the primers KU52-776R_Fw and M4, KU52-776R_Rv and B2f2108. A DNA fragment was then amplified from the two fragments by recombinant PCR using M4 and B2f2108, which was digested with *Sac*I-*Eco*RI and used to replace the corresponding region of pB2KU52 to construct pB2KU52^{776R}. pB2KU52^{776R2} was constructed essentially as described for pB2KU52^{776R} but using the primer pairs KU52-776R2_Fw and M4, KU52-776R2_Rv and B2f2108. pB2KU52^{776R4} was constructed essentially as described for pB2KU52^{776R} but using pB2KU52^{776R} as a template for recombinant PCR with the primer pairs KU52-776R4-2_Fw and M4, KU52-776R4-2_Rv and B2f2108. pB2KU52^{776R5} was constructed essentially as described for pB2KU52^{776R} but using pB2KU52^{776R4} as a template for recombinant PCR with the primer pairs KU52-776R5-2_Fw and M4, KU52-776R5-2_Rv and B2f2108.

2.3.5. pB2KU52^{784T}, pB2KU52^{784T2}

DNA fragments were amplified by PCR from pB2KU52 using the primers KU52-784T_Fw and M4, KU52-784T_Rv and B2f2108. A DNA fragment was then amplified from these two fragments by recombinant PCR using M4 and B2f2108, which was digested with *Sac*I-*Eco*RI and used to replace the corresponding region of pB2KU52 to construct pB2KU52^{784T}. pB2KU52^{784T2} was constructed essentially as described for pB2KU52^{784T} but using the primer pairs KU52-784T2_Fw and M4, KU52-784T2_Rv and B2f2108.

2.3.6. pB2KU52$^{776R+784T}$, pB2KU52^{3NC}

A small DNA fragment of pB2KU52 digested with *Eco*RI and *Stu*I was used to replace the corresponding region of pB2KF2^{S} to construct pB2KU52$^{776R+784T}$. A small DNA fragment of pB2KN2 digested with *Eco*RI and *Stu*I was used to replace the corresponding region of pB2KU52 to construct pB2KU52^{3NC}.

2.3.7. pB2KU52^{776K2}, pB2KU52^{776K3}

DNA fragments were amplified by PCR from pB2KU52 using the primers KU52-776K2_Fw and M4, KU52-776K2_Rv and B2f2108. A DNA fragment from these two fragments was then amplified by recombinant PCR using M4 and B2f2108, which was digested with *Sac*I-*Eco*RI and used to replace the corresponding region of pB2KU52 to construct pB2KU52^{776K2}. pB2KU52^{776K3} was constructed essentially as described for pB2KU52^{776K2} but using pB2KU52^{776K2} as a template for recombinant PCR with the primer pairs KU52-776K3-2_Fw and M4, KU52-776K3-2_Rv and B2f2108.

2.4. Virus infection tests in plants

2.4.1. Chenopodium quinoa

28-day-old *C. quinoa* plants were inoculated with BMV virions or in vitro transcripts. Four upper fully expanded leaves were dusted with carborundum (600 mesh, Nacalai, Japan) and mechanically inoculated with 5 µl/leaf of virions (0.6 µg/µl) or transcripts (0.2 µg/µl each of RNA1, 2, 3 transcripts). To study virus infection in plants, viral CP was detected by western blot analysis at 7 or 14 days post inoculation (dpi).

2.4.2. Rice

Leaves of *C. quinoa* inoculated with BMV in vitro transcripts as described above were harvested at 7 dpi and stored in 1.5-ml microtubes at -80°C as inocula for rice plants. 7-8-day-old rice seedlings, when the second leaf was the same size as the first leaf, were inoculated with inocula. Frozen *C. quinoa* leaves used as inocula were ground in the stock tube using a plastic pestle with 0.5-ml of sterilized DW, then mixed with carborundum (600 mesh, Nacalai, Japan) and mechanically inoculated onto rice leaves. To examine virus infection in plants, viral CP was detected by hammer bolt analysis (2.6.2) at 2 or 4 dpi, and ELISA analysis at 14 dpi.

2.5. Protoplast experiments

2.5.1. Chenopodium quinoa

For this experiment, the largest leaves of a 2-month-old *C. quinoa* were selected and scratched with a razor blade then soaked in enzyme solution [0.6 M mannitol, 1.0% cellulase RS (Yakult, Tokyo, Japan) and 0.5% macerozyme R-10 (Yakult), 10 mM $CaCl_2$, 5 mM MES (pH 5.7)] at 25 °C in the dark condition without shaking overnight. Protoplasts were collected through 4 layers of cheesecloth and selected on a 20% sucrose bed by centrifugation at 40 *g* for 3 min, and then washed twice with MMC solution [0.6 M mannitol, 10 mM $CaCl_2$, 5 mM MES (pH 5.7)] by centrifugation at 40 *g* for 3 min. The protoplasts ($2\text{-}5x10^5$) were concentrated in 0.1 ml of MMC and mixed well with in vitro transcripts of BMV RNAs (2.5 µg each of RNAs 1, 2 and 3) and 0.2 ml of freshly prepared polyethylene glycol (PEG) solution [40% PEG 4000 (#81240; Fluka, Germany) in DDW containing 0.2 M mannitol, 0.1 M $Ca(NO_3)_2$]. After 15 s, the suspension was diluted with 2 ml of MMC and kept on ice for 15 min. The protoplasts were then washed once with MMC and incubated in 0.5 ml incubation solution [0.6 M mannitol, 1xAoki solution (pH 6.5, Kroner and Ahlquist, 1992), 4 mM MES (pH 5.7), 200 µg/ml chloramphenicol] at 25°C under weak light for 24 hours.

2.5.2. Rice

Rice seeds were dehulled, sterilized with 2% sodium hypochlorite, rinsed with water and sown on 1/2 MS agar. After 8 days, developed rice leaves were cut with a razor blade and soaked in enzyme solution [0.6 M mannitol, 1.5% cellulase RS (Yakult) and 0.3% macerozyme R-10 (Yakult), 1 mM $CaCl_2$, 10 mM MES (pH 5.7), 0.1% BSA] in the dark condition and shaken at 40 rpm for 16 h (Bioshaker BR-23FP, Taitec). Protoplasts were collected through 45 µm nylon mesh and selected on a 20% sucrose bed by centrifugation at 80 *g* for 10 min, after that they were washed twice with MMg solution [0.4 M mannitol, 15 mM $CaCl_2$, 4 mM MES (pH 5.7)] with centrifugation at 170 *g* for 3 min. The protoplasts ($5x10^5$) were concentrated in 50 µl of MMg and well mixed with in vitro transcripts of BMV RNAs (2.5 µg each of RNAs 1, 2 and 3) and 50 µl of freshly prepared polyethylene glycol (PEG) solution [40% PEG 4000 (#81240; Fluka, Germany) in DDW containing 0.2 M mannitol, 0.1 M $Ca(NO_3)_2$]. After 15 seconds, the suspension was diluted with 0.5 ml of the dilution solution [0.4 M mannitol, 125 mM $CaCl_2$, 5 mM KCl, 5 mM glucose, 1.5 mM MES (pH 5.7)] and kept on ice for 15 minutes. The protoplasts were then washed once with dillution solution and incubated in 0.5 ml of W5 solution [154 mM NaCl, 125 mM $MgCl_2$, 5 mM KCl, 4 mM MES (pH 5.7)] at 25°C under weak light for 24 hours.

2.6. Analysis of viral proteins

2.6.1. Detection of BMV CP in rice using ELISA

At 14 dpi, upper leaves of rice were harvested as samples and soaked in 600 µL carbonate buffer (15 mM Na_2CO_3, 35 mM $NaHCO_3$, 0.1 g/L NaN_3) in Collection Microtube with Cap (19560 and 19566, Qiagen), which were then shaken with zirconia beads (5 mm in diameter) in TissueLyser II (QIAGEN, USA) for 10 min to disrupt the leaf tissue and release the proteins. BMV CP was detected using rabbit anti-BMV antiserum (Iwahashi et al., 2005) as the primary antibody, and alkaline phosphatase (AP)-conjugated anti-rabbit antibody as the secondary antibody. Finally, *p*-nitrophenylphosphoric acid disodium salt (Nacalai Tesque, Japan) dissolved in diethanolamine substrate buffer [diethanolamine 48.5 ml, DW 400 ml, $MgCl_2$ 50 mg, NaN_3 0.1 g] was used to visualize CP signals, which were measured at OD_{450} and quantified using a microplate reader (iMark, Bio-Rad, USA).

2.6.2. Hammer blot analysis

Inoculated rice leaves were harvested as samples and the sap was transferred to a piece of 3MM chromatography paper (Whatman, UK) using a hammer. The paper was immersed and shaken in 1% Triton X-100 for 30 min to remove the pigments from sap. BMV CP was then detected using rabbit anti-BMV antiserum as the primary antibody, and alkaline phosphatase (AP)-conjugated anti-rabbit antibody as the secondary antibody. Signals were visualized using NBT (nitro blue tetrazolium)/BCIP (5-bromo-4-chloro-3-indolyl phosphate) (Nacalai Tesque, Japan).

2.6.3. Western blot analysis

Total proteins were separated by electrophoresis on 15% polyacrylamide gels containing 0.1% SDS. Western blot analysis was performed as described (Damayanti et al., 1999), using polyvinylidene difluoride (PVDF) membranes (Immobilon-P; Millipore, Bedford, MA, USA). BMV CP was detected using rabbit anti-BMV antiserum as the primary antibody, and alkaline phosphatase (AP)-conjugated anti-rabbit antibody as the secondary antibody. Signals were visualized using NBT/BCIP.

2.7. Northern blot analysis

Northern blot analysis of total RNA was performed as described (Damayanti et al., 1999). Positive-strand RNAs of BMV were detected using digoxygenin-labeled T3 transcripts from *Hin*dIII-linearized pB3EH503, which contains the 0.2 kb *Hin*dIII/*Eco*RI fragment of pB3TP8 (Janda et al., 1987) in the *Hin*dIII/*Eco*RI site of pBluescriptII SK(-) (Stratagene, USA). Signals were visualized using CDP-Star (Roche) and detected using a luminescence image analyzer (LuminoGraph, Atto, Japan).

2.8. Yeast two-hybrid screening

Yeast two-hybrid (Y2H) screening was performed to identify BMV 2a protein-rice protein interactions, as essentially described (Hollenberg et al., 1995). The Y2H plasmids and cDNA library were kindly provided by Dr. K. Yamaguchi and T. Kawasaki, Kindai University.

2.8.1. Strains and plasmids

Saccharomyces cerevisiae strain L40 (ATCC, MYA-3332) was used as the host strain for the Y2H screening. The 2a gene fragments were cloned into pBTM116-GW (bait vector; Ichimaru et al., 2022), which expresses the protein as a fusion between the *E. coli* LexA DNA-binding domain (BD) and the BMV 2a protein fragment, N-terminal deleted 2a (△N, amino acids 162-822) or the C-terminal region of 2a (amino acids 697-822). Forward primers BTM-GW-bf2aNdel_Fw for N-terminal deleted 2a, and BTM-GW-bf2aC_Fw for the C-terminal fragment of 2a, were used together with the common reverse primer BTM-GW-bf2a_Rv.

After PCR amplification using pB2KU52 or pB2KU52$^{776R+784T}$ as a template, the amplified fragments were transferred into pBTM116-GW by the Gateway system using an LR clonase reaction with the pENTR/D-TOPO cloning kit (Thermo Fisher Scientific). A rice cDNA library constructed using poly (A)+ RNAs from rice cultured cells (Kawasaki et al., 2006), was kindly provided by K. Yamaguchi and T. Kawasaki, was used as a prey, allowing expression of potential interacting proteins as fusions with the transcriptional activation domain

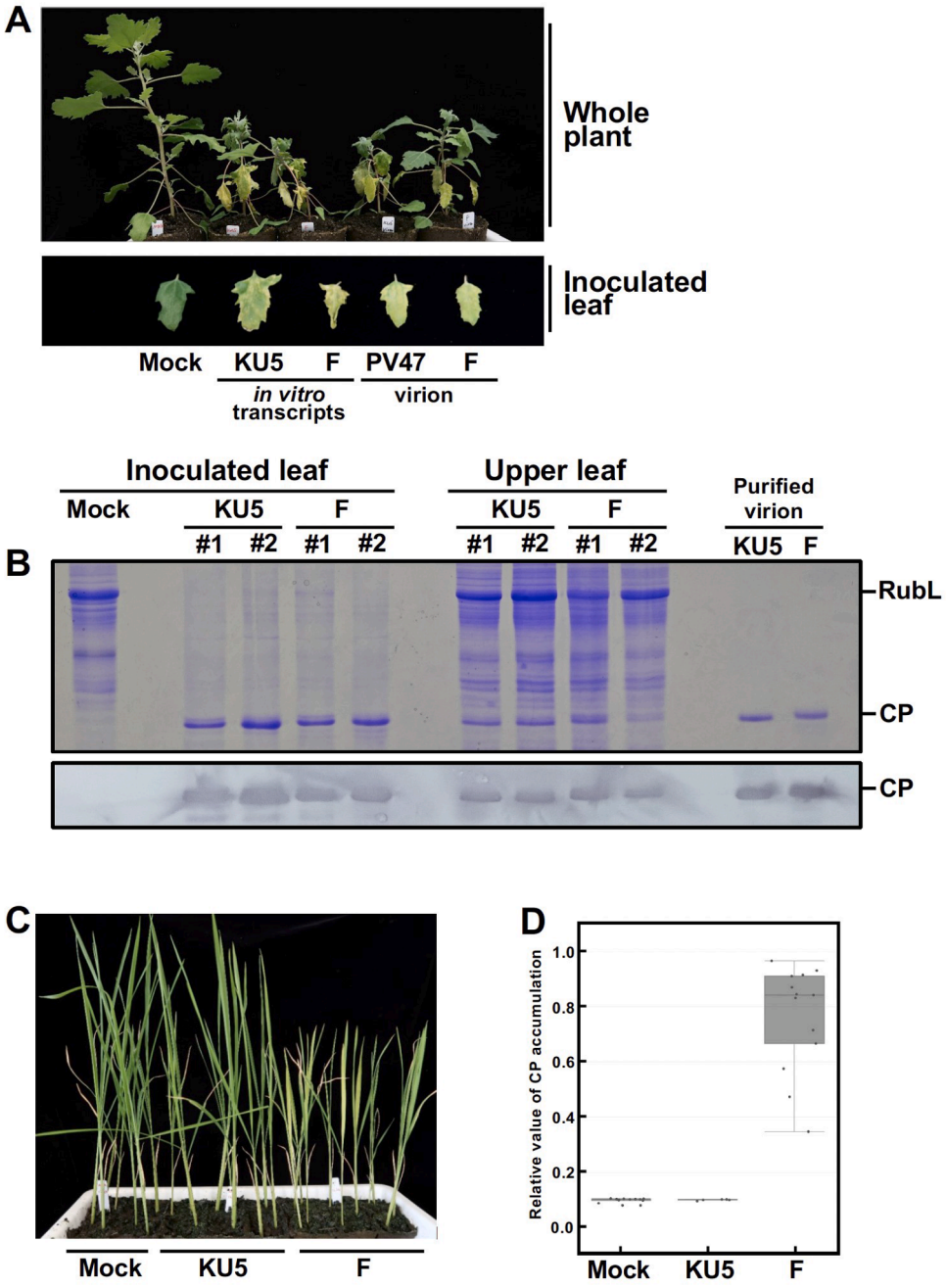

Fig. 1. Infectivity of BMV strains KU5 strain and F in *C. quinoa* and rice (cv.Habataki). (A) *C. quinoa* plants inoculated with BMV strains. ATCC_PV47 is the parental strain of KU5. *In vitro* transcripts from infectious cDNA clones for KU5 and F strains or purified virions of PV47 and F strains were used as inocula. At 14 days post inoculation, infected plants showed dwarfism and curled upper leaves. Inoculated leaves showed yellow lesions as one of the typical symptoms of BMV. (B) Western blotting of *C. quinoa* leaves inoculated with BMV F strain and KU5 strain to detect CP accumulation (lower panel). Leaves were excised as samples at 14 days after inoculation. Samples from two independent plants (#1 and #2) per inoculation were loaded together with 1 ng purified virion of KU5 strain and F strain. CP was detected with anti-BMV antiserum. Rubisco large subunit (RubL) was stained with Coomassie brilliant blue and used as a loading control (upper panel). (C) Rice plants inoculated with BMV F strain and KU5 strain. At 14 days post inoculation, F strain-inoculated rice showed dwarfism and yellowish leaves, whereas KU5 strain-inoculated rice was comparable to mock-inoculated plants. (D) Box plots showing the relative level of viral CP accumulation in upper leaves of rice by ELISA. Leaves were excised as samples at 14 dpi and CP was detected using anti-BMV antiserum. The box represents the interquartile range (IQR), encompassing the middle 50% of the data, with its lower and upper boundaries corresponding to the first quartile (Q1, 25th percentile) and third quartile (Q3, 75th percentile), respectively. The median (Q2, 50th percentile) is shown as a horizontal line within the box, representing the central tendency of the dataset. The whiskers extend beyond the box to indicate data variability, reaching the minimum and maximum values within 1.5 times the interquartile range (1.5 × IQR) from Q1 and Q3. The boxplots were generated using the CNSknowall platform (https://cnsknowall.com).

(AD) of the herpesvirus protein VP16.

2.8.2. Transformation and screening

The bait plasmid pBTM116-2a was transformed into L40 using the lithium acetate method. The transformed yeast cells were selected on synthetic dropout (SD) medium lacking tryptophan (SD/-Trp) to ensure the presence of the bait plasmid. The cDNA library was then introduced into the bait-containing yeast strain, and co-transformants were selected on SD medium lacking leucine and tryptophan (SD/-Leu/-Trp). To identify positive interactions, the transformed yeast cells were plated on high stringency SD medium lacking leucine, tryptophan, histidine (SD/-Leu/-Trp/-His/) and incubated at 30°C for 3–5 days.

2.8.3. Sequencing and validation

Plasmids from positive colonies were extracted, amplified in *E. coli*, and sequenced to identify interacting proteins. Candidate interactions were further validated by dilution experiments.

3. Results

3.1. Infectivity of the BMV strains KU5 and F in C. quinoa and rice

The BMV F strain was derived from infectious cDNA clones and originated from a novel isolate of *Festuca arundinacea* that, unlike previously characterized BMV strains, was reported to infect rice systemically (Ding et al., 2006). The KU5 strain was produced from infectious cDNA clones derived from ATCC_PV47 strain (the type strain of BMV,

A

		pseudorecombinants						
Strain	KU5	Rc1	Rc2	Rc3	Rc4	Rc5	Rc6	F
RNA1	KU5	KU5	KU5	KU5	F	F	F	F
RNA2	KU5	KU5	F	F	KU5	KU5	F	F
RNA3	KU5	F	KU5	F	KU5	F	KU5	F

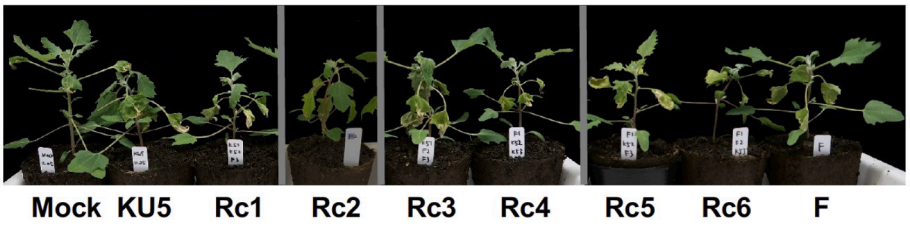

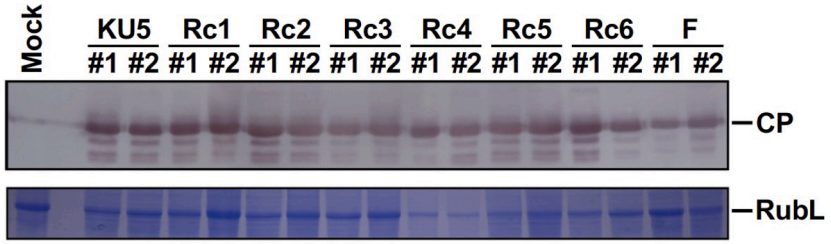

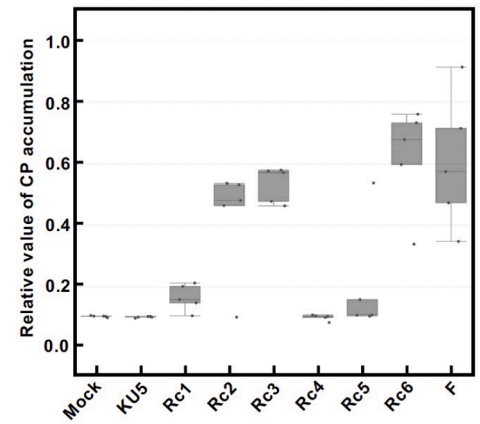

Fig. 2. Infectivity of pseudorecombinant BMV strains in *C. quinoa* and rice (cv. Habataki). (A) The different compositions of the pseudorecombinant strains are shown in the table. (B) *C. quinoa plants* inoculated with the pseudorecombinant strain. At 7 days post inoculation (dpi), infected plants showed dwarfism and distortion of the upper leaves. (C) Western blot of *C. quinoa* leaves inoculated with BMV recombinant strains to detect CP accumulation. Leaves were excised as samples 7 days after inoculation and viral CP was detected using anti-BMV antiserum. For others, see the legend to Fig. 1(B). (D) Infectivity assays where rice was inoculated with the pseudorecombinant strains shown in table (A). Systemic infection with BMV was determined by ELISA, which detects the accumulation of CP in the upper leaves of rice at 14 dpi.

ATCC). The *in vitro* transcripts of the KU5 strain and the virions of its parental strain PV47 showed similar infectivity in *C. quinoa* (Fig. 1A) and neither of them infected rice (Fig. 1C and data not shown), confirming that the KU5 strain recapitulates the biological properties of the PV47 strain.

To compare the infectivity of two BMV strains, KU5 and F, we first inoculated *C. quinoa* with *in vitro* transcripts. At 14 days post-inoculation (dpi), infected plants exhibited dwarfism and distorted upper leaves compared to mock-inoculated plants. The inoculated leaves also developed yellow lesions, a characteristic symptom of BMV infection (Fig. 1A). Systemic infection was further confirmed by western blot analysis of BMV coat protein (CP) accumulation in upper leaves (Fig. 1B). Infected *C. quinoa* leaves were then homogenized and used as an inoculum to infect rice (cv. Habataki). At 14 dpi, rice plants infected with the F strain showed dwarfism and yellowing of leaves, whereas those infected with the KU5 strain remained asymptomatic and were comparable to mock-inoculated plants (Fig. 1C). Systemic infection in rice was assessed by ELISA, which detected accumulation of BMV CP in the upper leaves of F strain-inoculated rice, but not in KU5 strain-inoculated plants (Fig. 1D). These results demonstrate that both the KU5 and F strains of BMV infect *C. quinoa* systemically, whereas only the F strain is capable of systemic infection in rice (cv. Habataki).

3.2. RNA2 of BMV determines BMV infectivity in rice

BMV has a tripartite RNA genome, RNAs 1, 2 and 3. To determine which segment plays a critical role in host specificity between the KU5 and F strains, pseudorecombinants with swapped RNA segments were generated using in vitro transcripts from infectious cDNA clones. The composition of pseudorecombinants Rc1 to Rc6 is shown in Fig. 2a, and their infectivity was assessed.

In *C. quinoa*, all six pseudorecombinants (Rc1 to Rc6), together with both parental strains, established systemic infection, as confirmed by symptom development and CP accumulation (Fig. 2b, c). However, their infectivity in rice was variable as assessed by ELISA. Pseudorecombinant strains Rc2, Rc3, and Rc6 not only achieved a higher frequency of systemic infection but also showed increased CP accumulation in the upper leaves of rice, compared to the other recombinant strains (Fig. 2d). Notably, all three strains contained RNA2 from strain F. In particular, the pseudorecombinant Rc2, which contained RNA1 and RNA3 from the KU5 strain and RNA2 from the F strain, showed that RNA2 from the F strain alone was sufficient to confer systemic infectivity in rice.

Conversely, pseudorecombinant strains Rc1, Rc4, and Rc5 carrying RNA2 from the KU5 strain showed significantly reduced infectivity in rice compared to the F strain. As the systemic infectivity of Rc1 and Rc5 was marginal, viral factors in RNA3 have only minor contribution to rice infectivity. These results indicate that among the three RNA segments, RNA2 is the critical determinant of BMV infectivity in rice.

3.3. Codons for 776R and 784T in RNA2 synergistically confer systemic infectivity of BMV in rice

To further refine the RNA2 region responsible for host specificity, several hybrid RNA2 constructs were generated by combining segments from KU5-RNA2 and F-RNA2. The composition of these hybrid RNA2 molecules is shown in Fig. S1A. Each hybrid RNA2 was co-inoculated with KU5-RNA1 and KU5 RNA3. In *C. quinoa*, all hybrid strains established a systemic infection (Fig. S1B, C). In rice, however, only hybrid strains B2KF2^{E} and B2KF2^{S} resulted in CP accumulation in the upper leaves (Fig. S1D, E), suggesting that the 3′-terminal region of RNA2 is critical for systemic infection in rice.

Sequence comparison of the 3′-terminal region of RNA2 between KU5 and F strains revealed three nucleotide differences, two of which were located in the coding region of the 2a gene. Specifically, the KU5 strain contained AAA (lysine) at codon 776 and GCA (alanine) at codon 784, whereas the F strain contained AGA (arginine) and ACA (threonine) at these positions.

To determine the precise viral factors at the nucleotide level, site-directed RNA2 mutagenesis was performed on KU5-RNA2, incorporating one or both of the F strain-specific codon changes (Fig. 3a). In *C. quinoa*, all mutant strains established systemic infection (Fig. 3b). However, in rice infectivity assays, ELISA analysis revealed that plants inoculated with KU5^{776R} or KU5^{784T}, which contained the F strain-specific arginine (R) at position 776 or threonine (T) at position 784, respectively, showed detectable CP accumulation in upper leaves, whereas the parental KU5 strain showed marginal CP accumulation. Notably, the KU5$^{776R+784T}$ double mutant exhibited even stronger infectivity than single mutants, with a higher infection frequency and consistently increased CP accumulation (Fig. 3C). These data suggest that the 776R and 784T codon changes in RNA2 are key determinants for systemic infection in rice, and their effects act synergistically to enhance BMV infectivity.

3.4. Codons for 776R and 784T influence long-distance movement of BMV in rice

To establish systemic infection, plant viruses undergo three major steps: replication in initially infected cells, cell-to-cell movement, and long-distance movement through the vasculature (Hipper et al., 2013). The BMV 2a protein, a polymerase protein, functions in conjunction with 1a and plays a critical role in viral RNA synthesis. Therefore, amino acid changes in 2a may affect RNA synthesis.

To assess the effect of RNA2 mutations on viral replication, *C. quinoa* and rice protoplasts were inoculated with BMV strains carrying mutant RNA2, together with RNA1 and RNA3 from strain KU5. Northern blot analysis was performed to analyze viral RNA accumulation. At 24 hours post-inoculation (hpi) in *C. quinoa* protoplasts, viral RNA levels were comparable among all strains tested, including the three mutants (KU5^{776R}, KU5^{784T}, and KU5$^{776R+784T}$) and the parental strains KU5 and F, indicating similar replication efficiency in *C. quinoa* cells (Fig. S2). In rice protoplasts, all mutant and parental strains accumulated to similar levels, with the KU5 strain even showing slightly higher viral RNA accumulation than the other strains (Fig. 4a). These results suggest that the two codon changes in RNA2 do not increase the efficiency of RNA replication.

To investigate the effect of these mutations on the second step of systemic infection - cell-to-cell movement - virus spread was analyzed in the inoculated rice leaves at 2 dpi and 5 dpi. KU5 RNA2 or mutant RNA2 (KU5$^{776R+784T}$) was co-inoculated with KU5 RNA1 and RNA3, and viral CP accumulation was immunodetected by hammer blotting. ImageJ quantification of the CP signal (Fig. 4b) showed an increase in average CP dot area from 2 dpi to 5 dpi (Fig. 4c), with no significant differences between the strains tested at 5 dpi (Fig. 4d). These results indicate that all BMV strains tested retained the comparable ability to spread between adjacent cells in rice leaves.

Since neither RNA replication nor cell-to-cell movement was significantly affected by the mutations at codons 776 and 784, these results suggest that the key role of these two nucleotide changes is to facilitate long-distance movement, thereby allowing systemic infection of KU5 strain in rice.

3.5. Amino acid changes, not RNA structure, are the main determinants on infectivity

For RNA viruses such as BMV, differences in infectivity can result from either direct changes in the RNA sequence or changes in the encoded amino acids. The RNA sequence itself can influence viral infectivity in several ways, including its role in the formation of RNA secondary structure, interactions with host factors, and susceptibility to RNA silencing (RNAi)-mediated defense mechanisms (Jeroen et al., 2014; Saurabh et al., 2014; Ding et al., 2007).

To determine whether the differences in infectivity at codons 776

A

RNA2	Infection rate (infected/inoculated)
F2	83.3% (20/24)
KU52	0% (0/24)
B2KU52^{776R}	81.3% (26/32)
B2KU52^{784T}	53.1% (17/32)
B2KU52$^{776R+784T}$	90.9% (20/22)

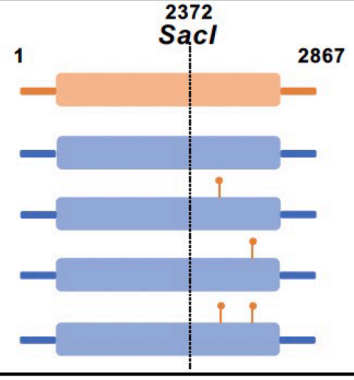

B

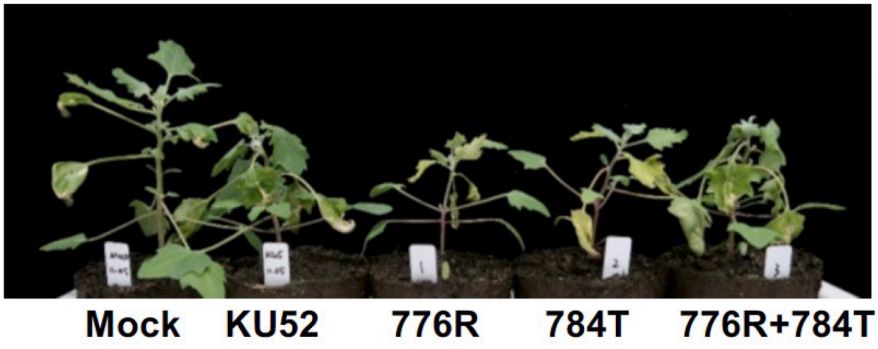

C

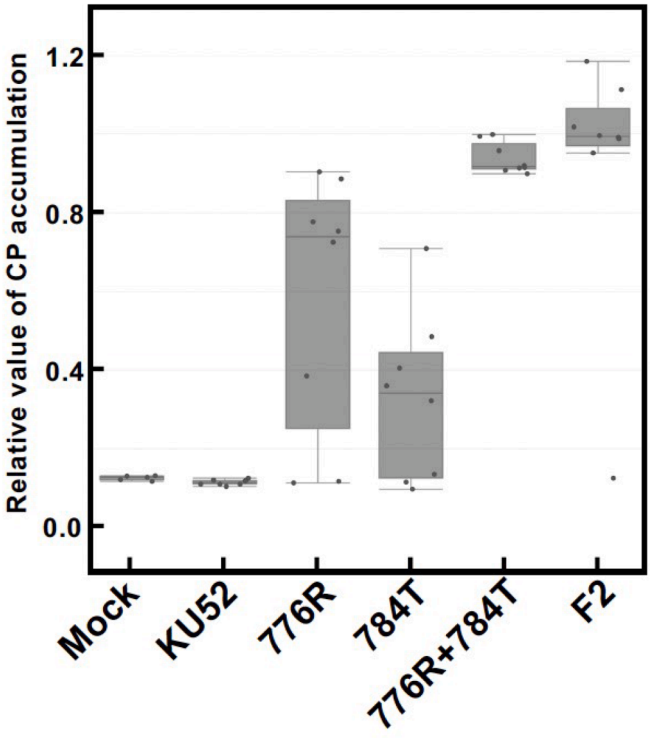

(caption on next page)

Fig. 3. Infectivity of BMV mutant strains in *C. quinoa* and rice. (A) Schematic representation of the RNA2 mutants and a summary of their infection rate in rice from 3 infectivity assays. Each RNA2 mutant was inoculated together with KU5 RNA1 and RNA3. Nucleotide numbers of border sites and a restriction site are shown. (B) *C. quinoa* plants inoculated with RNA2 mutants from (A). Each RNA2 mutant was inoculated together with KU5 RNA1 and RNA3. Images were taken at 7 days post inoculation (dpi). Infected plants showed dwarfism and distorted upper leaves. (C) Infectivity assays where rice (cv. Habataki) was inoculated with sap from *C. quinoa* leaves infected with the mutant strains shown in Table (A, B). Systemic infection with BMV was determined by ELISA, which detects the accumulation of CP in the upper leaves of rice at 14 dpi.

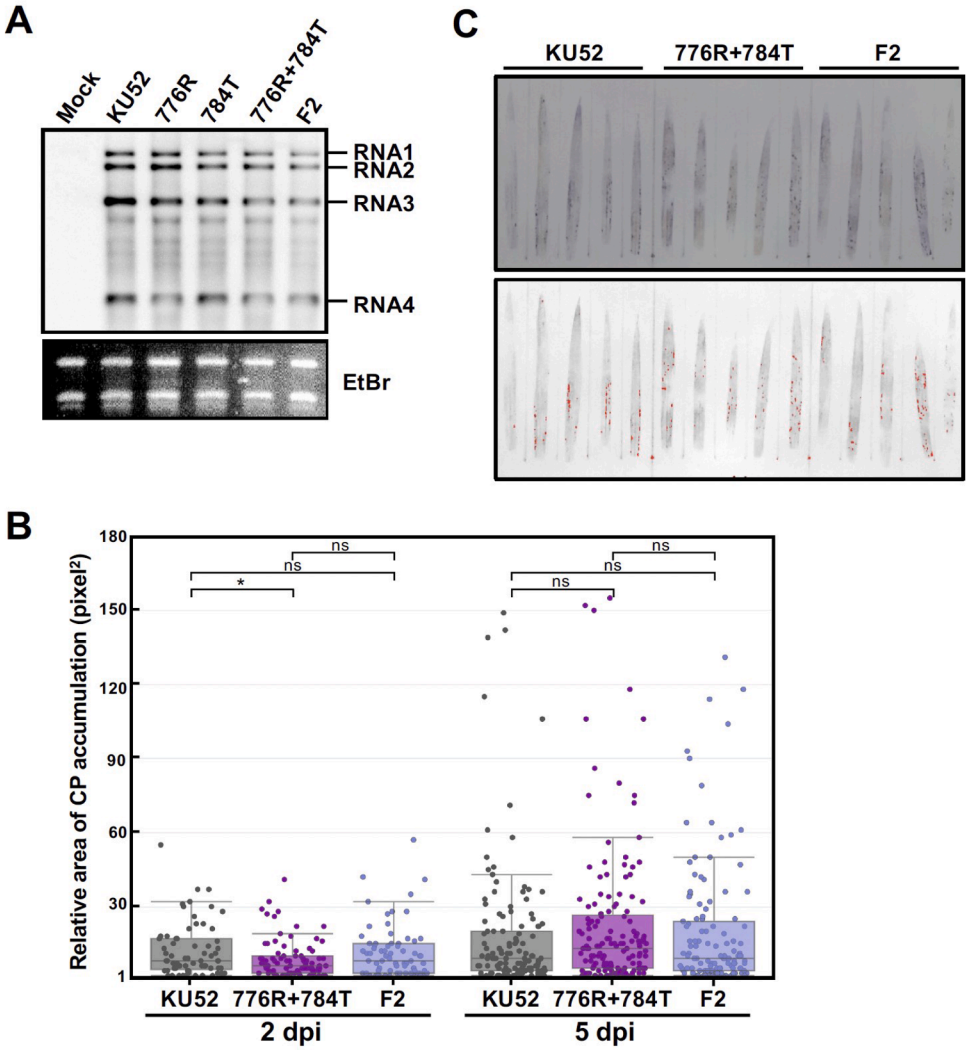

Fig. 4. Replication and short-range movement of mutant BMV strains. (A) Accumulation of viral RNA in rice protoplasts inoculated with in vitro transcripts of BMV mutant strains, KU5 strain and F strain at 24 h after inoculation. KU5 RNA2 (KU52), KU52^{776R} (776R), KU52^{784T} (784T), KU52$^{776R+784T}$ (776R+784T) or F RNA2 (F2) were used as inoculum together with KU5 RNA1 and RNA3. Viral RNAs were detected by Northern blot analysis using the BMV 3′ probe. EtBr-stained rRNA was used as a loading control. (B) Rice leaves were inoculated with KU5 RNA2 (KU52), KU52$^{776R+784T}$ (776R+784T) and F RNA2 (F2) together with KU5 RNA1 and RNA3. The relative area of BMV CP accumulation was determined by hammer blotting on the inoculated leaves at 2 dpi and 5 dpi using anti-BMV antiserum as in (C). An asterisk above the box plot denotes the results of a two-sample t-test between the connected groups, with the significance levels defined as follows: "*" indicates $p < 0.05$; "ns" (no significance) indicates $p > 0.05$. There were no significant differences between the 3 BMV strains ($P<0.05$) for the relative area of CP accumulation at 5 dpi. (C) A close-up picture of the hammer blot. Shown are the results of hammer blots at 5 dpi. The dark purple color (upper panel) was marked in red (lower panel) by ImageJ, and the red area upto 160 pixel^2 was picked up, measured for representing the area of CP accumulation and then quantified using ImageJ.

and 784 were due to RNA sequence variation, RNA secondary structure, or amino acid changes, RNA2 mutants with synonymous mutations were constructed. As shown in Fig. 5a, 776K2 (AAG) and 776R2 (CGC) encoded the same amino acids as 776K (lysine) and 776R (arginine), respectively, but had different RNA sequences. In addition, RNA structure predictions indicated that 776R formed a distinct 'stem' structure compared to 776K. To further investigate the potential role of RNA secondary structure, we designed two additional mutants: 776R4, which disrupted the stem structure in 776R, and 776K3, which introduced a stem structure similar to that of 776R. These mutants allowed us to assess whether the RNA structure affects systemic infection.

In this assay, we used purified virions from infected barley since preliminary tests indicated that all the mutants infected barley (cv. Hinodehadaka) plants (data not shown), a propagating host for BMV. Infectivity assays were then performed using purified virions at identical concentrations among the mutants. Systemic infection assays in rice revealed that only mutant strains containing arginine (R) at position 776 could establish systemic infection, whereas those retaining lysine (K) at this position failed to do so (Fig. 5b). Importantly, altering RNA sequence or secondary structure alone did not affect infectivity, as

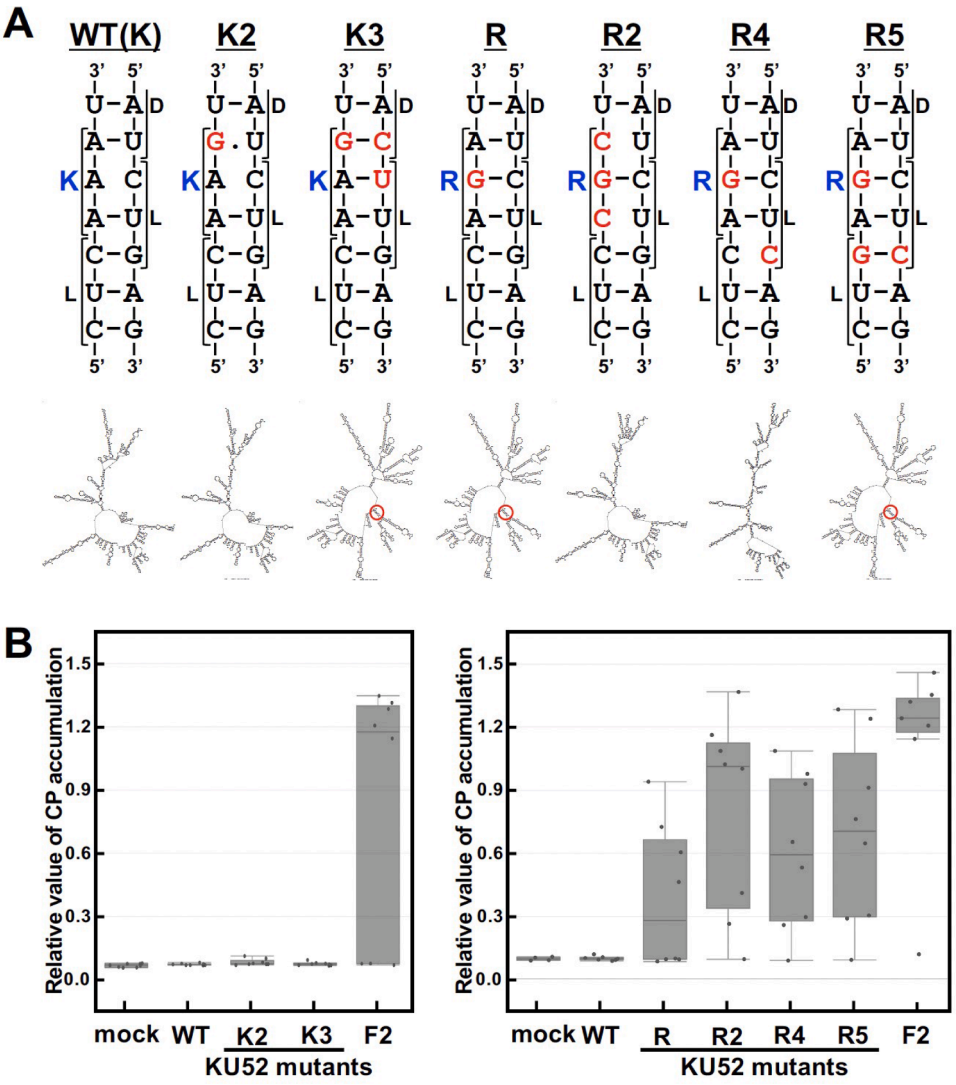

Fig. 5. Predicted RNA secondary structure and infectivity of BMV strains. (A) Nucleotide sequence and predicted RNA structure of RNA2 mutants. RNA folding structures were predicted for a folding temperature of 25C using the RNA folding form version 2.3 software (https://www.unafold.org). Due to the limitations of the software, only the 3′-terminal 1,000 nucleotide sequences were used for the prediction. RNA structures shown are predicted with the lowest delta G value (kcal/mol) in each mutant: K, -384.86; K2, -386.18; K3, -388.59; R, -388.88; R2, -389.29; R4, -385.07; R5, -388.88. Red circles indicate specific 'stem' structures in the target region shown above. Amino acid residues are shown with brackets next to the cocond, and those at position 776 are highlighted in blue. Mutated nucleotide residues are highlighted in red. (B) Systemic infectivity of BMV mutants propagated in barley was tested in rice (cv. Habataki). In vitro transcripts of wild-type and mutant KU5 RNA2 (KU52) and F RNA2 (F2) were used together with KU5 RNA1 and RNA3 as inocula in barley. All barley plants were successfully systemically infected with all inocula. All the mutants were purified from infected barley plants, the concentration of purified virions was adjusted to 0.4 mg/ml and the virions were used as inocula for rice. Upper leaves were excised as samples at 14 dpi and CP was detected by ELISA using anti-BMV antiserum.

neither the 776R4 nor 776K3 mutants showed changes in systemic infection ability. In support of this, the 776R5 mutant, which has a 'stem' structure like the 776R mutant, showed infectivity but did not exceed the infectivity of 776R2 without the stem similar to that in 776R. These results suggest that RNA secondary structure and sequence-dependent interactions with host factors do not play a major role in determining BMV infectivity in rice. Instead, the amino acid identity at these positions, particularly the presence of arginine at codon 776, is the primary determinant of systemic infection in rice.

3.6. The C-terminus of BMV-2a is an intrinsically disordered region (IDR) and interacts with several rice proteins

Viral proteins, especially those of RNA viruses, are often enriched in intrinsically disordered regions (IDRs; Tokuriki et al., 2009). These regions allow viral proteins to interact with a variety of host factors and serve as flexible linkers between functional domains, thereby contributing to viral adaptability (Xue et al., 2014). Computational predictions using I-TASSER (Zheng et al., 2021) and IUPred3 (Erdős et al., 2021) suggested that the C-terminal region of BMV-2a has features of an IDR (Figs. 6a, 6b), suggesting that this region may function in protein-protein interactions. Further predictions using AlphaFold 3 (Abramson et al., 2024) suggest that the C-terminal region is an IDR and lacks a stable three-dimensional structure (Fig. 6c). Interestingly, the two amino acids at positions 776 and 784 are located within the large alpha-helix of the predicted IDR. This alpha-helix may have the ability to interact with rice proteins. This may be supported by a previous report describing the function of the IDR to interact with multiple partner proteins (Ishino et al., 2014).

To investigate potential interactions between the 2a protein and host factors, a yeast two-hybrid (Y2H) screen was performed using an N-terminally truncated version of 2a [2a (ΔN region)] and the C-terminal region of 2a [2a (C-terminal)] as bait, with a rice cDNA library as prey. We chose such 2a fragments as baits in the Y2H assay for the following

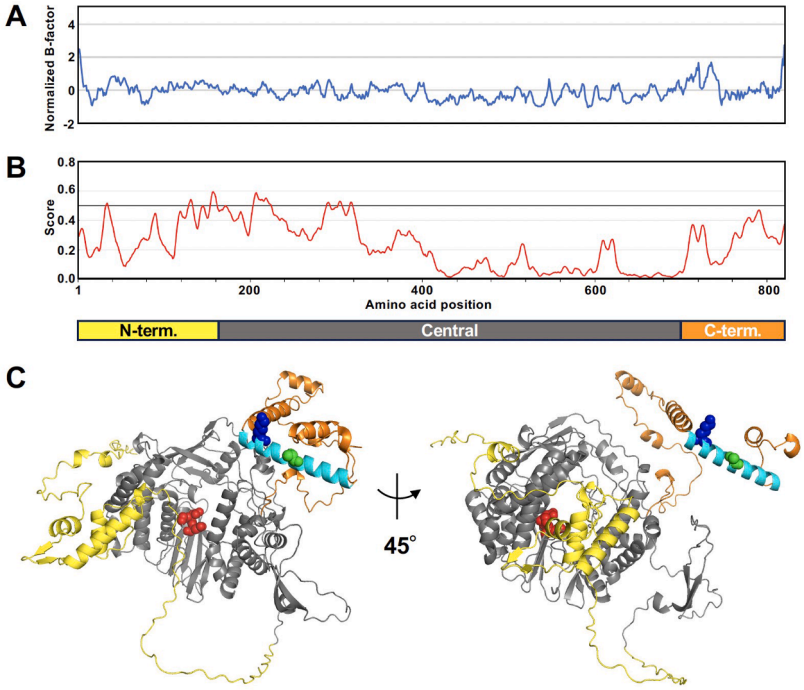

Fig. 6. The C-terminal region of BMV-2a may be an intrinsically disordered region. (A) Normalized B-factor score of BMV-KU5-2a predicted by I-TASSER (Zhang et al., 2022; https://zhanggroup.org/I-TASSER/). The B-factor is a value that indicates the degree of the inherent thermal mobility of residues/atoms in proteins. (B) Score of BMV-KU5-2a predicted by IUPred3 (Erdős et al., 2021; https://iupred3.elte.hu/), of which the C-terminal region of BMV-2a may be an intrinsically disordered region (IDR). (C) A 3D structure of the BMV-KU5 2a protein predicted by Alphafold3 (Abramson et al., 2024; https://alphafoldserver.com/). The N (aa 1-161) and C (aa 697-822) terminal non-conserved domains are colored yellow and orange, respectively. The central domain (aa 162-696) conserved in the RNA-dependent RNA polymerase (RdRP) is colored grey. The "GDD" triple amino acids conserved in RdRP and involved in its catalytic activity are highlighted in red. The 776th and 784th amino acids within the alpha-helix (cyan) in the C-terminal IDR predicted region are highlighted in blue and green, respectively. A pair of rotated structures are shown to visualize the key amino acids. Figures were generated using Pymol software (ver. 2.5.2).

reasons: (1) the rice cDNA library in our hand was constructed as fusions to the activation domain (Kawasaki et al., 2006); (2) the full- length 2a protein of BMV, when fused to the DNA-binding domain in the Y2H system, has been reported to show transcriptional activation in the absence of a fusion partner (O'Reilly et al., 1997); (3) our preliminary assay using the full-length 2a protein of the BMV KU5 strain also showed transcriptional autoactivation, but the two truncated 2a proteins (C-terminal and ΔN region) with essential amino acid residue polymorphism, did not (data not shown). The aim was to determine whether KU5-2a and mutant-2a have different interactions with rice proteins. As shown in Table 1, several rice proteins were identified as interaction partners of 2a (C-terminal) and 2a (ΔN region). Notably, the interaction patterns varied between these two protein regions, with identified host factors including TIFY domain protein 11d and the ADP-ribosylation factor AGD12, suggesting that the 2a C-terminal region may be involved in protein interactions. However, no significant differences were observed in the interaction profiles between KU5-2a and mutant-2a.

4. Discussion

In this study, we identified two key amino acid residues, R776 and T784, within the C-terminal region of the BMV 2a protein that are critical for systemic infection and host adaptation in rice. Our results demonstrate that amino acid identity, rather than RNA sequence or secondary structure, is the primary determinant of BMV infectivity in this host. In addition, we provide evidence that the C-terminal region of 2a functions as an intrinsically disordered region (IDR), which may

Table 1
Yeast two-hybrid screening and assay showing interactions between rice proteins and different BMV-2a protein fragments (N-terminal truncation [△N] and C-terminal fragment). Bait activities of 2a fragments in the screen are indicated by "√", where the 2a fragment baited each rice protein. Binding activities are shown from none (-), weak (+) to strong (++++), as estimated by the dilution assay in Y2H. KU5 and MUT represent the wild type and a mutant with mutation of 776R and 784T of the sKU5 2a protein, respectively.

Predicted rice protein	Bait activity in the screening				Binding activity with other constructs			
	△N		C-terminal		△N		C-terminal	
	KU5	MUT	KU5	MUT	KU5	MUT	KU5	MUT
Long chain acyl-CoA 4 like protein	-	√	-	-	++	++	-	-
vacuolar protein sorting-associated protein 2 homolog 2	-	√	-	√	++	++	+++	+++
ADP-ribosylation factor AGD12	-	√	-	-	+++	+++	-	-
NAC domain-containing protein	-	√	-	√	+	+	+++	+++
Meiotic F-BOX protein MOF-like	√	√	-	-	+++	+++	++++	++++
TIFY DOMAIN PROTEIN 11d	√	√	-	-	++++	++++	-	-
putative chloroplast RNA processing protein	-	-	-	√	-	-	+++	+++
ethylene-responsive transcription factor 8	-	-	-	-	-	-	++++	++++

facilitate interactions with multiple host factors and thereby contribute to viral movement and adaptation.

Contribution of 776R and 784T at C-terminal region of the 2a protein of BMV-F to viral systemic movement in rice remains to be clarified. Except for the future analyses on interactions between the 2a protein and host factors as discussed below, use of fluorescent protein expressing BMV vector, histochemical analysis using anti-BMV serum, or in situ hybridization targeting BMV RNAs could be helpful to identify a viral movement process in which both amino acids are involved.

Viruses have evolved specialized mechanisms to transport their RNA and RNA replication complexes. In general, two primary modes of viral transport have been described: (i) virions, which protect the genome within a capsid shell formed by coat protein (CP) subunits, and (ii) viral ribonucleoprotein (RNP) complexes, in which the viral genome associates with viral and/or cellular proteins (Lucas, 2006). Both forms have been reported in BMV transport (Gopinath & Kao, 2007). It is plausible that the 2a protein is incorporated into RNP complexes during BMV movement and interacts with specific host factors to facilitate RNP transport across cellular boundaries and enable long-distance movement. To date, several host proteins have been identified that are involved in RNA and protein trafficking through the phloem. For example, KNOTTED1 (KN1) mediates the selective plasmodesmal trafficking of RNAs and proteins (Lucas et al., 1995), while actin patch protein 1 (App1) can recognize BMV and, when overexpressed in *Nicotiana benthamiana*, inhibits systemic infection by BMV (Zhu et al., 2007). These factors warrant further investigation for possible interactions with the BMV 2a protein or other components of the RNP complex.

However, we did not identify host factors that differentially interact with KU5-2a and the mutant 2a protein. This limitation may be due to the use of a rice cDNA library derived from cultured rice cells, which may not fully capture the host factors involved in viral transport. A cDNA library derived from differentiated rice cells, which are actively involved in viral movement, may provide more relevant interactions. In addition, the target protein may be membrane-associated, posing a challenge for detection by yeast two-hybrid screening. Future studies using alternative methods, such as co-immunoprecipitation or proximity labeling (Qin et al., 2021), may be required to elucidate the host factors involved.

Interestingly, our analysis identified an RRACH (R=A or G, H=A, C, U) RNA methylation motif within the nucleotide sequence encoding R776 and T784. Our preliminary studies using m^6A RNA immunoprecipitation showed high levels of methylation in this region. Previous studies have shown that RNA methylation increases the stability and infectivity of wheat yellow mosaic virus in wheat (Zhang et al., 2022), whereas in Arabidopsis, RNA methylation reduces the infectivity of alfalfa mosaic virus (Martínez-Pérez et al., 2021). Whether the m^6A modification of BMV RNA2 affects infectivity in rice remains an open question. Future research should focus on generating BMV mutants with disrupted methylation motifs to assess their infectivity and stability in rice.

RNA viruses have high mutation rates, which, although often deleterious, can sometimes confer increased infectivity or an expanded host range. However, host-associated selective pressures can lead to cross-host fitness trade-offs, where increased viral fitness in a new host may come at the expense of fitness in the original host (Bedhomme et al., 2015; Kirchner and Roy, 2002; Woolhouse et al., 2001). In our study, although western blot analysis did not provide clear evidence, northern blotting suggested that the KU5 strain accumulated higher levels of viral RNA in rice protoplasts compared to other mutant strains or the F strain (Fig. 4a). This observation suggests that the reduced RNA replication capacity may be a trade-off for an expanded host range. Since the RNA-dependent RNA polymerase (RdRp) domain is located in the central region of the 2a protein (Ahlquist et al., 1984; Fig. 6), it remains unclear how amino acid changes in the C-terminal region affect RNA synthesis. The two key amino acid residues, 776R and 784T in the C-terminal region of the 2a protein, might be involved in the accumulation of viral RNA and counteraction to host defensive responses. Analyses of accumulation levels of viral RNA in whole rice plants and transcript levels of host resistance-related genes would provide new insights into a possibility such as host-virus interactions which affect viral systemic infection in rice. Further research, particularly into the dynamics of RNA replication, is needed to determine whether there exist fitness trade-offs exist between the KU5 and F strains. If confirmed, investigating the specific mutations that increase rice infectivity in the KU5 strain while decreasing infectivity in *C. quinoa* would be a compelling avenue for future study.

Declaration of generative AI and AI-assisted technologies in the writing process

During the preparation of this work the authors used “DeepL Write Pro” in order to improve the readability and language of the manuscript. After using this service, the authors reviewed and edited the content as needed abd take responsibility for the content of the published article.

CRediT authorship contribution statement

Yifan Zhang: Writing – review & editing, Writing – original draft, Methodology, Investigation, Formal analysis, Data curation. **Masanori Kaido:** Writing – review & editing. **Akira Mine:** Writing – review & editing. **Yoshitaka Takano:** Writing – review & editing. **Kazuyuki Mise:** Writing – review & editing, Supervision, Project administration, Methodology, Investigation, Funding acquisition, Data curation, Conceptualization.

Declaration of competing interest

All authors declare that they have no conpelling interests. There are no financial or personal relationships with other organizations that could influence the outcome of this research.

Acknowlegdements

This work was supported by a Grant-in-Aid for Scientific Research (B) (16H04881, 23K23611) KAKENHI. We thank X. S. Ding and Richard S. Nelson (The Noble Foundation, OK, USA) for providing the full-length cDNA clone plasmids originated from the BMV Fescue strain. We thank Masayoshi Teraishi (Plant Breeding Lab, Kyoto University, Japan) for rice (cv. Habataki) seeds. We also thank K. Yamaguchi and T. Kawasaki (Kindai University, Nara, Japan) for the rice cDNA library and plasmids for yeast two-hybrid screening.

Supplementary materials

Supplementary material associated with this article can be found, in the online version, at doi:10.1016/j.virusres.2025.199564.

Data availability

Data will be made available on request.

Refernces

Abramson, J., Adler, J., Dunger, J., Evans, R., Green, T., Pritzel, A., Ronneberger, O., Willmore, L., Ballard, A.J., Bambrick, J., Bodenstein, S.W., Evans, D.A., Hung, C.C., O'Neill, M., Reiman, D., Tunyasuvunakool, K., Wu, Z., Žemgulytė, A., Arvaniti, E., Beattie, C., Bertolli, O., Bridgland, A., Cherepanov, A., Congreve, M., Cowen-Rivers, A.I., Cowie, A., Figurnov, M., Fuchs, F.B., Gladman, H., Jain, R., Khan, Y.A., Low, C.M.R., Perlin, K., Potapenko, A., Savy, P., Singh, S., Stecula, A., Thillaisundaram, A., Tong, C., Yakneen, S., Zhong, E.D., Zielinski, M., Žídek, A., Bapst, V., Kohli, P., Jaderberg, M., Hassabis, D., Jumper, J.M., 2024. Accurate structure prediction of biomolecular interactions with AlphaFold 3. Nature 630, 493–500. https://doi.org/10.1038/s41586-024-07487-w.

Ahlquist, P., Dasgupta, R., Kaesberg, P., 1984. Nucleotide sequence of the brome mosaic virus genome and its implications for viral replication. J. Mol. Biol. 172, 369–383. https://doi.org/10.1016/S0022-2836(84)80012-1.

Ahlquist, P., French, R., Janda, M., Loesch-Fries, L.S., 1984. Multicomponent RNA plant virus infection derived from cloned viral cDNA. Proc. Natl. Acad. Sci. USA 81, 7066–7070. https://doi.org/10.1073/pnas.81.22.7066.

Allison, R., Thompson, C., Ahlquist, P., 1990. Regeneration of a functional RNA virus genome by recombination between deletion mutants and requirement for cowpea chlorotic mottle virus 3a and coat genes for systemic infection. Proc. Natl. Acad. Sci. USA 87, 1820–1824. https://doi.org/10.1073/pnas.87.5.1820.

Bedhomme, S., Hillung, J., Elena, S.F., 2015. Emerging viruses: why they are not jacks of all trades? Curr. Opin. Virol. 10, 1–6. https://doi.org/10.1016/j.coviro.2014.10.006.

Chen, J., Ahlquist, P., 2000. Brome mosaic virus polymerase-like protein 2a is directed to the endoplasmic reticulum by helicase-like viral protein 1a. J. Virol. 74, 4310–4318. https://doi.org/10.1128/jvi.74.9.4310-4318.2000.

Damayanti, T.A., Nagano, H., Mise, K., Furusawa, I., Okuno, T., 1999. Brome mosaic virus defective RNAs generated during infection of barley plants. J. Gen. Virol. 80, 2511–2518. https://doi.org/10.1099/0022-1317-80-9-2511.

Ding, X.S., Schneider, W.L., Chaluvadi, S.R., Mian, M.R., Nelson, R., 2006. Characterization of a Brome mosaic virus strain and its use as a vector for gene silencing in monocotyledonous hosts. Mol. Plant-Microbe Interact. 19, 1229–1239. https://doi.org/10.1094/MPMI-19-1229.

Ding, X.S., Rao, C.S., Nelson, R.S., 2007. Analysis of gene function in rice through virus-induced gene silencing. Methods Mol. Biol. 354, 145–160. https://doi.org/10.1385/1-59259-966-4:145.

Erdős, G., Pajkos, M., Dosztányi, Z., 2021. IUPred3: prediction of protein disorder enhanced with unambiguous experimental annotation and visualization of evolutionary conservation. Nucleic. Acids. Res. 49, W297–W303. https://doi.org/10.1093/nar/gkab408.

Gopinath, K., Kao, C.C., 2007. Replication-independent long-distance trafficking by viral RNAs in Nicotiana benthamiana. Plant Cell 19, 1179–1191. https://doi.org/10.1105/tpc.107.050088.

He, G., Zhang, Z., Sathanantham, P., Diaz, A., Wang, X., 2021. Brome mosaic virus (Bromoviridae). Encyclopedia Virol. 3, 252–259. https://doi.org/10.1016/B978-0-12-809633-8.21294-6.

Hipper, C., Brault, V., Ziegler-Graff, V., Revers, F., 2013. Viral and cellular factors involved in phloem transport of plant viruses. Front. Plant Sci. 4, 154. https://doi.org/10.3389/fpls.2013.00154.

Hodge, B.A., Salgado, J.D., Paul, P.A., Stewart, L.R., 2019. Characterization of an Ohio isolate of brome mosaic virus and its impact on the development and yield of soft red winter wheat. Plant Dis. 103, 1101–1111. https://doi.org/10.1094/PDIS-07-18-1282-RE.

Hollenberg, S.M., Sternglanz, R., Cheng, P.F., Weitraub, H., 1995. Identification of a new family of tissue-specific basic helix-loop-helix proteins with a two-hybrid system. Mol. Cell Biol. 15, 3813–3822. https://doi.org/10.1128/MCB.15.7.3813.

Ichimaru, K., Yamaguchi, K., Harada, K., Nishio, Y., Hori, M., Ishikawa, K., Inoue, H., Shigeta, S., Inoue, K., Shimada, K., Yoshimura, S., Takeda, T., Yamashita, E., Fujiwara, T., Nakagawa, A., Kojima, C., Kawasaki, T., 2022. Cooperative regulation of PBI and MAPKs controls WRKY45 transcription factor in rice immunity. Nat. Commun. 13, 2397. https://doi.org/10.1038/s41467-022-30131-y.

Ishino, S., Yamagami, T., Kitamura, M., Kodera, N., Mori, T., Sugiyama, S., Ando, T., Goda, N., Tenno, T., Hiroaki, H., Ishino, Y., 2014. Multiple interactions of the intrinsically disordered region between the helicase and nuclease domains of the archaeal Hef protein. J. Biol. Chem. 289, 21627–21639. https://doi.org/10.1074/jbc.M114.554998.

Iwahashi, F., Fujisaki, K., Kaido, M., Okuno, T., Mise, K., 2005. Synthesis of infectious in vitro transcripts from Cassia yellow blotch bromovirus cDNA clones and a reassortment analysis with other bromoviruses in protoplasts. Arch. Virol. 150, 1301–1314. https://doi.org/10.1007/s00705-005-0500-6.

Janda, M., French, R., Ahlquist, P., 1987. High efficiency T7 polymerase synthesis of infectious RNA from cloned brome mosaic virus cDNA and effects of 5' extensions on transcript infectivity. Virology 158, 259–262. https://doi.org/10.1016/0042-6822(87)90265-0.

Jeroen, W., Richard, B., Joris, J.M., Nora, M., David, J.E., Peter, S., 2014. The influence of viral RNA secondary structure on interactions with innate host cell defences. Nucleic. Acids. Res. 42, 3314–3329. https://doi.org/10.1093/nar/gkt1291.

Kamer, G., Argos, P., 1984. Primary structural comparison of RNA-dependent polymerases from plant, animal and bacterial viruses. Nucleic. Acids. Res. 12, 7269–7282. https://doi.org/10.1093/nar/12.18.7269.

Kawasaki, T., Koita, H., Nakatsubo, T., Hasegawa, K., Wakabayashi, K., Takahashi, H., Umemura, K., Umezawa, T., Shimamoto, K., 2006. Cinnamoyl-CoA reductase, a key enzyme in lignin biosynthesis, is an effector of small GTPase Rac in defense signalling in rice. Proc. Natl. Acad. Sci. USA. 103, 230–235. https://doi.org/10.1073/pnas.0509875103.

Kirchner, J., Roy, B., 2002. Evolutionary implications of host–pathogen specificity: fitness consequences of pathogen virulence traits. Evol. Ecol. Res. 4, 27–48. https://doi.org/10.1023/A:1011647526731.

Kroner, P., Ahlquist, P., 1992. RNA-based viruses. S.J. Gurr, M.J. McPherson, D.J. Bowles (Eds.), Molecular Plant Pathology: A Practical Approach, vol. 1, Oxford University Press, New York (1992), pp. 23–34.

Lucas, W.J., 2006. Plant viral movement proteins: agents for cell-to-cell trafficking of viral genomes. Virology. 344, 169–184. https://doi.org/10.1016/j.virol.2005.09.026.

Lucas, W.J., Bouché-Pillon, S., Jackson, D.P., Nguyen, L., Baker, L., Ding, B., Hake, S., 1995. Selective trafficking of KNOTTED1 homeodomain protein and its mRNA through plasmodesmata. Science (1979) 270, 1980–1983. https://doi.org/10.1126/science.270.5244.1980.

Martínez-Pérez, M., Gómez-Mena, C., Alvarado-Marchena, L., Nadi, R., Micol, J.L., Pallas, V., Aparicio, F., 2021. The m^6A RNA demethylase ALKBH9B plays a critical role for vascular movement of alfalfa mosaic virus in Arabidopsis. Front. Microbiol. 12, 745576. https://doi.org/10.3389/fmicb.2021.745576.

Miller, W.A., Dreher, T.W., Hall, T.C., 1985. Synthesis of brome mosaic virus subgenomic RNA in vitro by internal initiation on (-)-sense genomic RNA. Nature 313, 68–70. https://doi.org/10.1038/313068a0.

Mise, K., Ahlquist, P., 1995. Host-specificity restriction by bromovirus cell-to-cell movement protein occurs after initial cell-to-cell spread of infection in nonhost plants. Virology. 206, 276–286. https://doi.org/10.1016/S0042-6822(95)80043-3.

O'Reilly, E.K., Paul, J.D., Kao, C.C., 1997. Analysis of the interaction of viral RNA replication proteins by using the yeast two-hybrid assay. J. Virol. 71, 7526–7532. https://doi.org/10.1128/jvi.71.10.7526-7532.1997.

Qin, W., Cho, K.F., Cavanagh, P.E., 2021. Deciphering molecular interactions by proximity labeling. Nat. Methods 18, 133–143. https://doi.org/10.1038/s41592-020-01010-5.

Sacher, R., Ahlquist, P., 1989. Effects of deletions in the N-terminal basic arm of brome mosaic virus coat protein on RNA packaging and systemic infection. J. Virol. 63, 4545–4552. https://doi.org/10.1128/jvi.63.11.4545-4552.1989.

Saurabh, S., Vidyarthi, A.S., Prasad, D., 2014. RNA interference: concept to reality in crop improvement. Planta 239, 543–564. https://doi.org/10.1007/s00425-013-2019-5.

Schwartz, M., Chen, J., Janda, M., Sullivan, M., den Boon, J., Ahlquist, P., 2002. A positive-strand RNA virus replication complex parallels form and function of retrovirus capsids. Mol. Cell 9, 505–514. https://doi.org/10.1016/s1097-2765(02)00474-4.

Tokuriki, N., Oldfield, C.J., Uversky, V.N., Berezovsky, I.N., Tawfik, D.S., 2009. Do viral proteins possess unique biophysical features? Trends. Biochem. Sci. 34, 53–59. https://doi.org/10.1016/j.tibs.2008.10.009.

Traynor, P., Young, B.M., Ahlquist, P., 1991. Deletion analysis of brome mosaic virus 2a protein: effects on RNA replication and systemic spread. J. Virol. 65, 2807–2815. https://doi.org/10.1128/JVI.65.6.2807-2815.199.

Trzmiel, K., Zarzyńska-Nowak, A., Hasiów-Jaroszewska, B., 2023. Biological properties, genetic structure and molecular variability of brome mosaic virus population. Plant Pathol. 72, 1293–1304. https://doi.org/10.1111/ppa.13757.

Woolhouse, M.E., Taylor, L.H., Haydon, D.T., 2001. Population biology of multihost pathogens. Science (1979) 292, 1109–1112. https://doi.org/10.1126/science.1059026.

Xue, B., Blocquel, D., Habchi, J., Uversky, A.v., Kurgan, L., Uversky, V.N., Longhi, S., 2014. Structural disorder in viral proteins. Chem. Rev. 114, 6880–6911. https://doi.org/10.1021/cr4005692.

Zhang, T., Shi, C., Hu, H., 2022. N6-methyladenosine RNA modification promotes viral genomic RNA stability and infection. Nat. Commun. 13, 6576. https://doi.org/10.1038/s41467-022-34362-x.

Zheng, W., Zhang, C., Li, Y., Pearce, R., Bell, E.W., Zhang, Y., 2021. Folding non-homology proteins by coupling deep-learning contact maps with I-TASSER assembly simulations. Cell Rep. Methods 1, 100014. https://doi.org/10.1016/j.crmeth.2021.100014.

Zhu, J., Gopinath, K., Murali, A., Yi, G., Hayward, S.D., Zhu, H., Kao, C., 2007. RNA-binding proteins that inhibit RNA virus infection. Proc. Natl. Acad. Sci. USA 104, 3129–3134. https://doi.org/10.1073/pnas.0611617104.